Carbon Nanotube–Ferrocene Hybrids

Single-Wall Carbon Nanotube–Ferrocene Nanohybrids: Observing Intramolecular Electron Transfer in Functionalized SWNTs**

Dirk M. Guldi, Massimo Marcaccio, Demis Paolucci, Francesco Paolucci,* Nikos Tagmatarchis, Dimitrios Tasis, Ester Vázquez, and Maurizio Prato**

Dedicated to Professor Dan Meyerstein
on the occasion of his 65th birthday

Since their discovery, carbon single-wall nanotubes (SWNTs) have drawn considerable attention, not only due to their unique chemical and physical properties, but also because of their promise in the area of materials chemistry.[1] A central aspect of nanotube chemistry, which yet awaits exploration, is their functionality and performance in donor–acceptor ensembles. Our recent success in SWNT functionalization,[2] based on the 1,3-dipolar cycloaddition of azomethine ylides to the double bonds of SWNTs, led us to pursue the covalent linkage of an electron donor, namely ferrocene, to the all-carbon network. Here we report for the first time on intramolecular electron transfer reactions in a novel SWNT-based donor–acceptor ensemble.

The SWNTs were produced by Carbon Nanotechnology, Inc., by the HIPco process (http://cnanotech.com). The functionalized SWNTs were synthesized by following our recently published procedure.[2] Accordingly, *N*-functionalized glycines **1a,b** and paraformaldehyde were heated to

---

[*] Dr. D. M. Guldi
Radiation Laboratory
University of Notre Dame
Notre Dame, IN 46556 (USA)
Fax: (+1) 574-631-8068
E-mail: guldi.1@nd.edu

Prof. Dr. F. Paolucci, Dr. M. Marcaccio, Dr. D. Paolucci
Dipartimento di Chimica "G. Ciamician"
Università di Bologna
Via Selmi 2, 40126 Bologna (Italy)
Fax: (+39) 051-2099-456
E-mail: paolucci@ciam.unibo.it

Prof. Dr. M. Prato, Dr. N. Tagmatarchis, Dr. D. Tasis, Dr. E. Vázquez
Dipartimento di Scienze Farmaceutiche
Università di Trieste
Piazzale Europa 1, 34127 Trieste (Italy)
Fax: (+39) 040-52-572
E-mail: prato@units.it

[**] This work was carried out with partial support from the EU (RTN networks "FUNCARS" and "CASSIUSCLAYS"), MIUR (PRIN 2002, nos. 2002032171 and 2002035735), the Universities of Trieste and Bologna, and the Office of Basic Energy Sciences of the U.S. Department of Energy. This is document NDRL-4468 from the Notre Dame Radiation Laboratory. We thank Mr. Claudio Gamboz and Prof. Maria Rosa Soranzo (CSPA, Trieste) for kind help with the TEM experiments. SWNT = single-wall nanotube.

Supporting information for this article is available on the WWW under http://www.angewandte.org or from the author.

© 2003 Wiley-VCH Verlag GmbH & Co. KGaA, Weinheim DOI: 10.1002/ange.200351289

130 °C in dimethylformamide in which SWNTs were suspended (Scheme 1). After five days, the solvent was evaporated under reduced pressure, and the residue was washed several times with diethyl ether. (See Supporting Information for experimental details.)

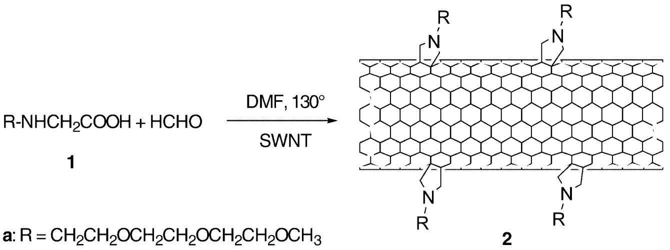

a: R = $CH_2CH_2OCH_2CH_2OCH_2CH_2OCH_3$
b: R = $CH_2CH_2OCH_2CH_2OCH_2CH_2NHCOFc$
Fc = ferrocenyl

Scheme 1. Synthesis of functionalized SWNTs.

Whereas SWNTs **2a** were identical to those reported recently,[2] the newly synthesized SWNTs **2b** were soluble in most organic solvents without sonication. They were characterized by common analytical techniques, such as FTIR, UV/Vis, and ^1H NMR spectroscopy, and transmission electron microscopy (TEM). In the ^1H NMR spectrum, the pyrrolidine and ethylenedioxy protons ($\delta = 2$–4 ppm) gave rise to rather broad peaks, whereas the ferrocenyl protons ($\delta = 4.7$, 4.3, 4.2 ppm) retained their fine structure. Therefore, since the ferrocenyl groups are rather remote from the SWNT core, it is reasonable to assume that they are less affected by the π-electron cloud of the SWNT. In the FTIR spectrum, the characteristic absorptions of the amide bond of **2b** at 1725 and 1667 cm^{-1} are present.

Differential scanning calorimetry (DSC) showed a loss of 25 wt % when a sample of SWNT **2b** was heated to 350 °C. This is in full agreement with the extent of functionalization we found earlier in **2a**, that is, approximately one ferrocene group per hundred carbon atoms of the SWNT (see Supporting Information for experimental details).[2,3]

The transmission electron micrograph of **2b** (Figure 1) shows functionalized SWNTs in relatively thin bundles. This bundling is a consequence of the way in which the TEM grid is prepared for the experiments. For the deposition of SWNTs we use diethyl ether, a solvent that does not dissolve **2a** and **2b** well and thus keeps the SWNT in bundles, which are easier to identify under the microscope.

The UV/Vis spectrum of **2b** in dichloromethane showed a broad band around 250 nm, which monotonically decreases in intensity with increasing wavelength, and shoulders at 326 and 431 nm. The observed absorbance is linearly dependent on the concentration of the measured sample, that is, no aggregation of the organic functionalized nanotubes takes place. Since the absorption cross section of ferrocene in the visible region is much smaller than that of the SWNTs, the absorption spectra of **2a** and **2b** are virtually identical. However, the most important characteristic of functionalized SWNT **2a,b** is the absence of appreciable near-IR (NIR) band-gap transitions (van Hove singularities), which is a clear indication of functionalization.[2,3]

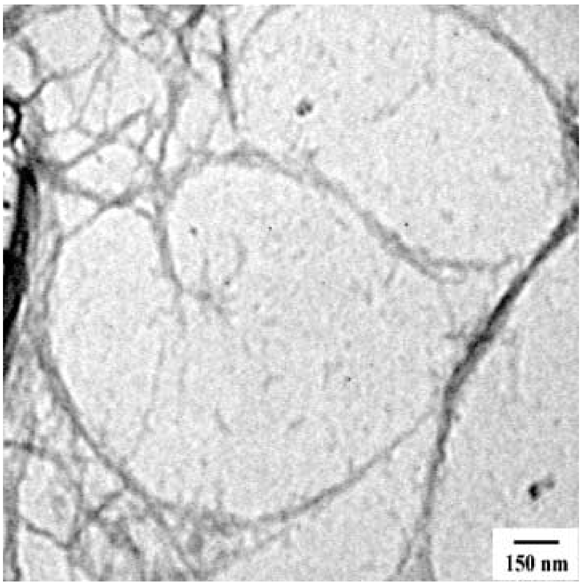

Figure 1. TEM image of SWNTs **2b**.

The cyclic voltammetric (CV) curve of **2b** (see Supporting Information) shows a reversible oxidation peak with $E_{1/2} = +0.53$ V, which results from diffusion-controlled $Fc \rightarrow Fc^{\bullet +}$ oxidation. No discrete redox steps, associated with a single-electron charge transfer in SWNT, were evident in CV or differential-pulse voltammetric experiments. The CV curve was instead characterized by a continuous increase in current with potential, indicative of multiple-electron charge transfers, similar to those reported in recent work.[4] The onset of reduction of the functionalized SWNTs is at around −0.5 V. Thus, the lowest energy level of $(SWNT)^{\bullet -}$–$(Fc)^{\bullet +}$ is expected to lie around 1.0 eV. Owing to the low-lying $(SWNT)^{\bullet -}$–$(Fc)^{\bullet +}$ state, **2b** can be considered a promising material for photo-induced electron transfer.

For electron-transfer interactions in photoexcited SWNTs, changes in fluorescence[5] and transient absorption served as sensitive and meaningful probes. As mentioned above, the weak absorption of the ferrocene units led us to focus primarily on the deactivation of SWNTs (**2a**,**b**) excited with light of different wavelengths.[6]

For the SWNT band gap fluorescence in the range 800–2000 nm, some interesting observations were made. The room-temperature fluorescence of SWNT–TEG (**2a**) in dichloromethane with excitation at 355 nm is depicted in Figure 2. Several transitions are discernable, some in the form of well-resolved strong bands, while others appear as bands with lower oscillator strength and/or shoulders. Light scattering, as a possible origin of the NIR transitions, was ruled out by probing various excitation wavelengths (i.e., 300–550 nm). Overall, the NIR transitions lack the remarkable fine structure reported recently for individual, isolated nanotubes of different diameters.[7] It is possible that the extensive functionalization obtained in our case strongly affects the properties of the excited state and the band-gap fluorescence of the SWNTs, with concomitant loss of fine structure in the absorption spectrum.[2,3,8]

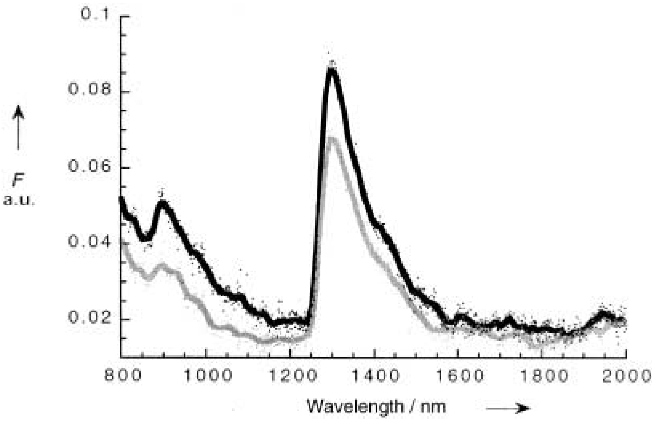

Figure 2. Fluorescence spectra of SWNT–TEG (**2a**; black) and SWNT–Fc (**2b**; gray) in deoxygenated dichloromethane following excitation at 355 nm. The optical density at the excitation wavelength ($OD_{355\,nm}$ = 0.5) was matched to obtain comparable fluorescence spectra.

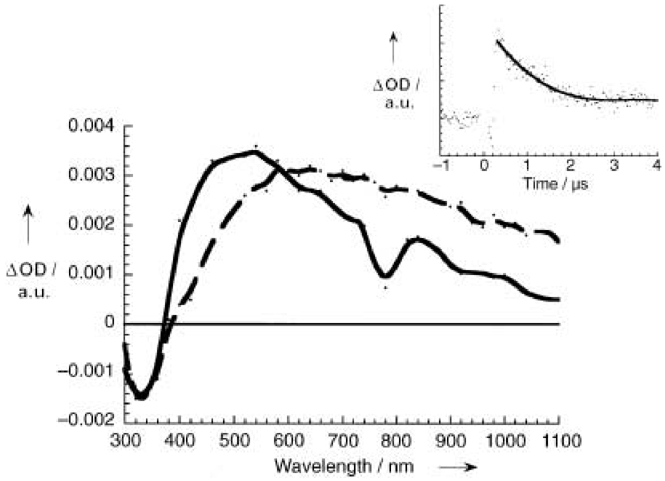

Figure 3. Transient absorption spectrum (UV/Vis/NIR part) of SWNT–TEG (**2a**; dashed spectrum) and SWNT–Fc (**2b**; solid spectrum) in deoxygenated dichloromethane, recorded 50 ns after a 355 nm laser pulse (8 ns), which shows the characteristic features of photoexcited SWNTs with $\lambda_{max} \approx 650$ nm and a (SWNT)$^{\bullet-}$ fingerprint with $\lambda_{max} \approx 500$ nm. The inset shows the decay of (SWNT)$^{\bullet-}$–(Fc)$^{\bullet+}$ at 450 nm.

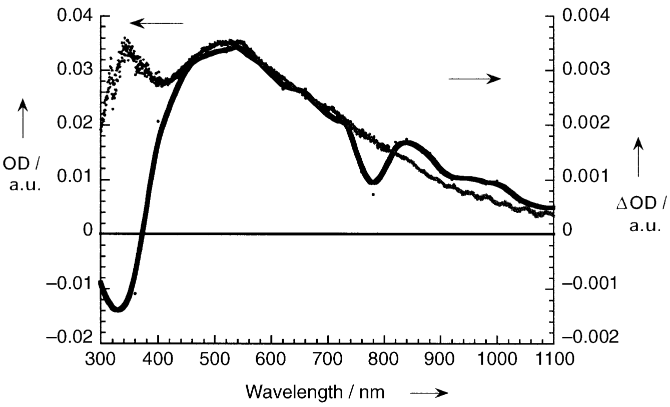

Figure 4. Absorption spectrum recorded after bulk electrolysis at −1.8 V of SWNT–Fc (**2b**), overlaid with the transient absorption spectrum following photoexcitation of **2b** (see also Figure 3). Experimental conditions: Bu_4NPF_6 (0.05 M), saturated THF solution, $T = -32$ °C, working electrode: Pt, quartz OTTLE cell with a 0.03 cm path length.

The fluorescence in SWNT–Fc (**2b**), in a sample that displays matching absorbances at the 350 nm excitation wavelength to **2a**, is quenched relative to that in **2a**. While the high-energy bands (i.e., <1000 nm) give rise to about 50% quenching, the quenching of the corresponding low-energy bands (>1300 nm) is more moderate, with an efficiency of only about 25%. The different excited-state energies are primarily responsible for this trend, since the driving force for an intramolecular electron transfer ($-\Delta G_{ET}$) is markedly reduced in the lower energy region.[9]

To gather evidence for possible quenching of electron transfer, as opposed to intrinsically faster deactivation of the excited state in **2b** (0.2 ns),[9] we carried out transient absorption spectroscopy with dichloromethane solutions of **2a** and **2b**. On laser excitation of **2a**, a long-lived transient ($\tau = 20$ µs) was observed, the features of which are displayed in Figure 3. This intermediate decayed quantitatively to the ground state in the absence and presence of molecular oxygen (O_2) without involving the formation of singlet oxygen ($^1O_2$). This finding implies that the energy of the excited state is too low for reaction with molecular oxygen, a hypothesis that was corroborated by the lack of $^1O_2$ phosphorescence.

Figure 3 also displays the transient obtained on irradiation of **2b** in solution. Clearly, the spectrum is different from that of **2a**, especially in the range between 375 and 500 nm, where the transient for **2a** shows minimal absorption changes. This leads us to postulate intramolecular electron transfer to give (SWNT)$^{\bullet-}$–(Fc)$^{\bullet+}$. The analysis of the decay component of (SWNT)$^{\bullet-}$–(Fc)$^{\bullet+}$ throughout the 400–700 nm region yields a lifetime of 1110 ± 100 ns (see inset to Figure 3).

With the aid of bulk electrolysis and pulse radiolysis the formation of the reduced SWNT in (SWNT)$^{\bullet-}$–(Fc)$^{\bullet+}$ was confirmed. In particular, bulk electrolysis at an applied potential of −1.8 V and pulse-radiolytic reduction with hydrated electrons (e_{aq}^-) led to the formation of a species whose UV/Vis/NIR absorption is identical to that reported in Figure 3, and thus confirms the assignment to (SWNT)$^{\bullet-}$. Figure 4 shows the UV/Vis/NIR spectrum recorded after exhaustive bulk electrolysis of **2b** at −1.8 V. The spectrum shows a very broad band in the visible region, centered at 445 nm.[10] The pristine absorption spectrum was recovered upon re-oxidation (at 0 V), showing the reversibility of the reduction process on the timescale of the electrolysis experiment. Similarly, radiolytic reduction with e_{aq}^- led to differential absorption changes which closely resemble those seen in the photolytic and electrolytic experiments with a maximum (450 nm) and a shoulder (550 nm). The spectra of the radiolytically and photolytically generated species are shown in the Supporting Information.

To resolve the dynamics of formation of photoexcited SWNT-TEG and (SWNT)$^{\bullet-}$–(Fc)$^{\bullet+}$, we used picosecond laser spectroscopy. The transient spectra recorded 50 ps after laser excitation of **2a** are compared with those of **2a** and **2b** at a time delay of 4000 ps in the Supporting Information. Importantly, the two spectra at 4000 ps are qualitative matches to those recorded with a time delay of 50 ns, as displayed in Figure 3. In **2a**, the species is formed with a time constant of 1.65 ± 0.1 ns, while in **2b** the kinetics give rise to a much faster formation (0.28 ± 0.05 ns), which corresponds to an electron transfer rate of $3.6 \times 10^9\,s^{-1}$.

In summary, we have succeeded for the first time in demonstrating photoinduced electron transfer within a novel SWNT–ferrocene nanohybrid. The photoexcitation of SWNT–Fc with visible light leads to electron transfer that yields a long-lived $SWNT^{\bullet-}$–$Fc^{\bullet+}$ species, the spectral features of which were confirmed by steady-state electrolysis and time-resolved pulse radiolysis. These results, and especially the slow kinetics of charge recombination, appear promising in light of further developments of SWNT–Fc nanohybrids in solar-energy conversion.

Received: February 27, 2003 [Z51289]
Published Online: July 28, 2003

Keywords: carbon · electron transfer · fluorescence · nanotechnology · nanotubes

---

[1] a) Special issue on carbon nanotubes *Acc. Chem. Res.* **2002**, *35*, 997; b) J. L. Bahr, J. M. Tour, *J. Mater. Chem.* **2002**, *12*, 1952–1958; c) A. Hirsch, *Angew. Chem.* **2002**, *114*, 1933–1939; *Angew. Chem. Int. Ed.* **2002**, *41*, 1853–1859.

[2] a) V. Georgakilas, K. Kordatos, M. Prato, D. M. Guldi, M. Holzinger, A. Hirsch, *J. Am. Chem. Soc.* **2002**, *124*, 760–761; b) V. Georgakilas, N. Tagmatarchis, D. Pantarotto, A. Bianco, J.-P. Briand, M. Prato, *Chem. Commun.* **2002**, 3050–3051.

[3] V. Georgakilas, D. Voulgaris, E. Vázquez, M. Prato, D. M. Guldi, A. Kukovecz, H. Kuzmany, *J. Am. Chem. Soc.* **2002**, *124*, 14318–14319.

[4] L. Kavan, P. Rapta, L. Dunsch, M. J. Bronikowski, P. Willis, R. E. Smalley, *J. Phys. Chem. B* **2001**, *105*, 10764–10771.

[5] a) J. E. Riggs, Z. Guo, D. L. Carroll, Y.-P. Sun, *J. Am. Chem. Soc.* **2000**, *122*, 5879–5880; b) Y.-P. Sun, B. Zhou, K. Henbest, K. F. Fu, W. J. Huang, Y. Lin, S. Taylor, D. L. Carroll, *Chem. Phys. Lett.* **2002**, *351*, 349–353; c) Y. Sun, S. R. Wilson, D. I. Schuster, *J. Am. Chem. Soc.* **2001**, *123*, 5348–5349.

[6] The emission in the visible region—see for example earlier work by Sun et al.[5]—exhibited no quenching when comparing **2a** and **2b** with matching absorbances at the excitation wavelength. Similarly, no changes were noted in the underlying radiative lifetime (approximately 3.0 ns).

[7] a) M. J. O'Connell, S. M. Bachilo, C. B. Huffman, V. C. Moore, M. S. Strano, E. H. Haroz, K. L. Rialon, P. J. Boul, W. H. Noon, C. Kittrell, J. P. Ma, R. H. Hauge, R. B. Weisman, R. E. Smalley, *Science* **2002**, *297*, 593–596; b) S. M. Bachilo, M. S. Strano, C. Kittrell, R. H. Hauge, R. E. Smalley, R. B. Weisman, *Science*, **2002**, *298*, 2361–2366; c) A. Hagen, T. Hertel, *Nano Lett.* **2003**, *3*, 383–388.

[8] Excitation of the 890 and 1300 nm fluorescence transitions led to rather poorly resolved spectra with a series of broad maxima. For example, for the emission maximum at 890 nm excitation maxima were found at 440 nm, 600 nm, and 790 nm.

[9] The radiative decay constants were determined for both **2a** and **2b** by time-resolved fluorescence measurements. By following the emission up to 850 nm (i.e., the upper limit of our strobe detection system) we noticed that the lifetime, which in **2a** is about 1.8 ns and agrees well with published data,[6] is substantially shorter in **2b** (major component of 0.2 ns).

[10] Similar features were obtained on electrolysis of **2a** (see Supporting Information). The spectroelectrochemical experiments were carried out in a quartz OTTLE cell with a 0.03 cm path length.

© 2003 Wiley-VCH Verlag GmbH & Co. KGaA, Weinheim